# A Fluorescence-Based Alkaline Phosphatase-Coupled Polymerase Assay for Identification of Inhibitors of Dengue Virus RNA-Dependent RNA Polymerase

**Article** *in* Journal of Biomolecular Screening · February 2011

DOI: 10.1177/1087057110389323 · Source: PubMed



**6 authors**, including:

Pornwaratt Niyomrattanakit

**26** PUBLICATIONS **1,451** CITATIONS

SEE PROFILE

Pei-Yong Shi

Novartis

**359** PUBLICATIONS **15,320** CITATIONS

SEE PROFILE

Yen-Liang Chen

Novartis

**24** PUBLICATIONS **1,684** CITATIONS

SEE PROFILE

# A Fluorescence-Based Alkaline Phosphatase–Coupled Polymerase Assay for Identification of Inhibitors of Dengue Virus RNA-Dependent RNA Polymerase

Pornwaratt Niyomrattanakit, Siti Nurdiana Abas, Chin Chin Lim, David Beer, Pei-Yong Shi and Yen-Liang Chen

*J Biomol Screen* 2011 16: 201 originally published online 10 January 2011
DOI: 10.1177/1087057110389323

# A Fluorescence-Based Alkaline Phosphatase–Coupled Polymerase Assay for Identification of Inhibitors of Dengue Virus RNA-Dependent RNA Polymerase

PORNWARATT NIYOMRATTANAKIT, SITI NURDIANA ABAS, CHIN CHIN LIM, DAVID BEER, PEI-YONG SHI, and YEN-LIANG CHEN

The flaviviral RNA-dependent RNA polymerase (RdRp) is an attractive drug target. To discover new inhibitors of dengue virus RdRp, the authors have developed a fluorescence-based alkaline phosphatase–coupled polymerase assay (FAPA) for high-throughput screening (HTS). A modified nucleotide analogue (2′-[2-benzothiazoyl]-6′-hydroxybenzothiazole) conjugated adenosine triphosphate (BBT-ATP) and 3′UTR-$U_{30}$ RNA were used as substrates. After the polymerase reaction, treatment with alkaline phosphatase liberates the BBT fluorophore from the polymerase reaction by-product, $BBT_{PPi}$, which can be detected at excitation and emission wavelengths of 422 and 566 nm, respectively. The assay was evaluated by examining the time dependency, assay reagent effects, reaction kinetics, and signal stability and was validated with 3′dATP and an adenosine-nucleotide triphosphate inhibitor, giving $IC_{50}$ values of 0.13 μM and 0.01 μM, respectively. A pilot screen of a diverse compound library of 40,572 compounds at 20 μM demonstrated good performance with an average Z factor of 0.81. The versatility and robustness of FAPA were evaluated with another substrate system, BBT-GTP paired with 3′UTR-$C_{30}$ RNA. The FAPA method presented here can be readily adapted for other nucleotide-dependent enzymes that generate PPi. (*Journal of Biomolecular Screening* 2011;16:201-210)

**Key words:** HTS, NS5, RNA-dependent RNA polymerase, dengue virus, FAPA

## INTRODUCTION

DENGUE FEVER IS ONE OF THE MOST IMPORTANT human mosquito-borne viral diseases endemic in tropical countries where there is an urgent need to develop specific and effective therapeutic drugs. Several antiviral compounds, such as ribavirin, mycophenolic acid, geneticin, 7-deaza-2′-C-methyl-adenosine, 7-deaza-2′-C-acetylene-adenosine, and 6-O-butanoyl castanospermine, have demonstrated in vitro efficacy against dengue virus (DENV) replication and in animal viremia models.[1-7] However, no specific antidengue medication is available on the market.

The flavivirus NS5 protein contains both methyltransferase and RNA-dependent RNA polymerase activities that are essential for viral propagation.[8-10] The N-terminal 1-272 amino acids form the S-adenosyl-L-methionine-dependent methyltransferase domain, which methylates the RNA cap to form N7-methyl-guanosine and 2′-O-methyl adenosine, resulting in a structure similar to the mammalian mRNA cap.[10,11] The C-terminal part of NS5 (residues 273-900) encodes the RNA-dependent RNA polymerase responsible for synthesizing RNA copies of both plus and minus polarity.[12] The DENV-3 NS5 RNA-dependent RNA polymerase (RdRp) structures, both in apo and nucleotide-complexed forms, have been determined,[13] enabling rational drug design and potentially aiding inhibitor development. The absence of RdRp activity in host cells makes it an attractive target for antiviral drug development.

Several reports have described the identification of flavivirus NS5 inhibitors using high-throughput screening (HTS) as the starting point. The assays are usually based on radioactivity (e.g., scintillation proximity assays in solid phase).[4,14] We have previously developed a DENV RdRp scintillation proximity assay for HTS using [$^3$H]GTP and poly(C)/oligo($G)_{20}$ as the substrate and RNA template, respectively, resulting in the identification of an N-sulfonylanthranilic acid inhibitor with an $IC_{50}$ at 0.7 μM.[4] However, the drawbacks of radioactive assays are requirements for safety precautions and potential harm to both the scientists and environment. To identify novel inhibitors of DENV RdRp with a different readout, we report here the development of a fluorescence-based polymerase assay (FAPA) with improved robustness. The method is similar to the polymerase assay reported by Bhat et al.[15] and Kozlov et al.[16] To achieve a robust assay suitable for HTS, several parameters, including optimal assay buffer components, enzyme/

Novartis Institute for Tropical Diseases, Chromos, Singapore.

Received Jul 15, 2010, and in revised form Sep 27, 2010. Accepted for publication Oct 1, 2010.

Supplementary material for this article is available on the *Journal of Biomolecular Screening* Web site at http://jbx.sagepub.com/supplemental.

Journal of Biomolecular Screening 16(2); 2011
DOI: 10.1177/1087057110389323

substrate ratios, reaction times, signal stability, and reaction kinetics, were investigated. The signal-to-noise (S/N) ratio and Z factor were used to evaluate the robustness and reproducibility of the assay. The assay was validated by $IC_{50}$ determination using a specific adenosine nucleotide triphosphate analogue and 3′dATP as inhibitors. A pilot screen consisting of 40,572 compounds in 384-well plates was used to determine the performance of the assay. Our FAPA has proved to be feasible and suitable for HTS for inhibitor finding, with a Z factor of 0.8. In addition to assay development for compound screening, we also evaluated FAPA with an additional nucleotide-RNA substrate system comprising BBT-GTP and 3′UTR-$C_{30}$. The versatility of FAPA was demonstrated by evaluating it with other NS5 RdRp enzymes from DENV-2 and 3. Our results indicate that FAPA is widely adaptable for the development of assays for nucleotide-dependent enzymes that generate PPi, such as polymerases and transferases.

## MATERIALS AND METHODS

Common assay reagents and enzymes used in molecular cloning were purchased from Sigma-Aldrich (St. Louis, MO), Fisher Scientific (Waltham, MA), Roche Diagnostics (Indianapolis, IN), Stratagene (La Jolla, CA), Invitrogen (Carlsbad, CA), and New England Biolabs (Ipswich, MA). AttoPhos® kit was purchased from Promega (Madison, WI). QIAamp viral RNA mini kit, Qiagen plasmid maxi kit, QIAguick gel extraction kit, and QIAquick PCR purification kit were purchased from Qiagen (Valencia, CA). Superscript III reverse transcription kit and Zero Blunt TOPO PCR cloning kits were from Invitrogen. BBT-ATP and BBT-GTP were synthesized by and purchased from Jena Bioscience GmbH (Jena, Germany). The 3′dATP and 3′dGTP were purchased from Trilink Biotech (San Diego, CA), and RNA substrates 3′UTR-$U_{30}$ (5′-bio-$U_{30}$-AACAGGUUCU*AGAACCU GUU*-3′) and 3′UTR-$C_{30}$ (5′-bio-$C_{30}$-AACAGGUUCU*AGAAC CUGUU*-3′) were purchased from Dharmacon (Lafayette, CO). These hairpin self-priming RNAs contain 30 nucleotide-long incorporation regions fused with the 3′UTR sequence (negative strand in italics, complementary positive strand underlined). The dNTP mix was purchased from Roche Diagnostics, and 96- and 384-well black plates were from Corning Costar (Corning, NY). BBT fluorescence was monitored by either Tecan SafireII or Infinite® M1000 plate reader (Tecan, Durham, NC). The compound library used in this study contained compounds that were selected for structural diversity and for adhering to Lipinski's rule-of-5 and were obtained from various companies.

### *DENV NS5 cloning and expression*

Total RNA was extracted from tissue culture media supernatant containing D4MY01-22713 virus using the QIAamp Viral RNA kit following the manufacturer's instructions. The purified RNA was reverse-transcribed with Superscript III using the primer 5′-CAATGGTCTCTTTGGTGTTTG-3′. After reverse transcription, the primers 5′-CATATGGCTAGCGGA ACTGGGACCACAGGA-3′ and 5′-GCGGCCGCTTACA GAACTCCTTCACTCTC-3′ were used to amplify D4MY01-22713 NS5. The amplified PCR band was subsequently cloned into a zero blunt TOPO PCR cloning vector. After verification of the DNA sequence, the TOPO vector was cut with *NheI* and *NotI* restriction enzymes to release the DENV-4 NS5 fragment and cloned into pET28a cut with the same enzymes. DENV-2 NS5 (NGC strain) and DENV-3 (D3MY00-22366 strain) were cloned with similar procedures. The ligation reaction was transformed into Top10 cells (Invitrogen). Protein expression and purification were performed as previously described.[13] The recombinant protein was stored in 20 mM Tris-HCl (pH 7.0), 500 mM NaCl, 10% glycerol, and 10 mM 2-mercaptoethanol at −80 °C until use.

### *Optimization of alkaline phosphatase reaction on AttoPhos® polymerase by-product mimic*

The phosphatase hydrolysis reaction by calf intestinal alkaline phosphatase (CIP) on AttoPhos® (2′-[2-benzothiazoyl]-6′-hydroxybenzothiazole phosphate [$BBT_{Pi}$]; Promega)[17] was optimized in a 10-µL reaction containing 0.1 to 0.2 µM AttoPhos®, 0.1 to 10 nM CIP in 10 to 500 mM deoxyethanolamine (DEA), 200 mM NaCl, and 25 mM $MgCl_2$. The reaction was incubated at room temperature, and the release of BBT was continuously monitored at ex/em 422/566 nm for up to 16 h.

### *BBT-ATP utilization by DENV-4 NS5 RdRp, time course, buffer optimization, and kinetics*

The RNA template, 3′UTR-$U_{30}$ or 3′UTR-$C_{30}$, was resuspended to 200 µM in a buffer consisting of 50 mM Tris-Cl (pH 8.0) and 150 mM NaCl in 0.1% diethyl pyrocarbonate (DEPC) water. The solution was incubated at 55 °C to 60 °C for 5 min and placed at room temperature to allow the formation of the intramolecular hairpin. Polymerase activity was investigated with 50 nM NS5 in a time course experiment in 50 mM Tris-HCl (pH 7.0), 2 mM dithiothreitol (DTT), 10 mM KCl, and 1 mM $MnCl_2$ in a 30-µL reaction in a 96-well, half-well plate with either 20 or 100 nM RNA and 2 µM BBT-ATP. At intervals ranging from 0 to 300 min, 20 µL of stop buffer (200 mM NaCl, 25 mM $MgCl_2$, 1.5 M DEA) containing 25 nM CIP was added to terminate the NS5 polymerase reaction and to allow hydrolysis of $BBT_{PPi}$ by CIP. The released BBT was monitored after a 1-h incubation.

The optimization of the NS5 and RNA concentrations was carried out in 30-µL reactions in 96-well, half-well plates. Reactions containing 2.5 to 50 nM NS5 were tested with 10, 20, or 50 nM of RNA at a constant BBT-ATP concentration of 2 µM. The buffer composition was optimized by investigating the effect of 0 to 300 mM NaCl or KCl, 0 to 16 mM $MgCl_2$, 0% to 0.03% (w/v) Triton X-100, 0 to 5 mM DTT, 0% to 10% (v/v) DMSO, and different pH ranging from 6 to 10. The $K_m$ values

for RNA and BBT-ATP substrates were determined in optimized buffer (50 mM Tris-Cl [pH 7.0], 0.01% Triton X-100, 1 mM $MnCl_2$). The $K_m$ value for RNA was calculated with varying 3′UTR-$U_{30}$ RNA concentration from 1.25 to 80 nM (at a fixed BBT-ATP concentration of 20 μM), whereas the BBT-ATP $K_m$ value was measured by varying the concentration from 0.3 to 20 μM in the reactions containing 80 nM of 3′UTR-$U_{30}$ RNA. The $K_m^{app}$ value for 3′UTR-$U_{30}$ was determined in the presence of 2 μM BBT-ATP, and the $K_m^{app}$ for BBT-ATP was obtained with a fixed concentration of 50 nM 3′-UTR-$U_{30}$ RNA under similar assay conditions.

The enzyme stability was assessed using NS5 alone or by preincubation with either BBT-ATP or 3′UTR-$U_{30}$ RNA in 15 μL of the optimized assay buffer for 0 to 4 h at room temperature. Reactions were started by adding 15 μL of the remaining substrates at 2× concentration. Reactions were quenched at 60 min with 20 μL of stop buffer containing CIP and further incubated for 1 h at room temperature to allow complete hydrolysis by the phosphatase. The release of the BBT was monitored as described.

### *Assay validation with reference compounds 3'dATP and adenosine nucleotide triphosphate analogues*

The chain terminator 3′dATP and a triphosphorylated DENV NS5 RdRp nucleotide inhibitor (tpNITD008)[6] were used as reference compounds to validate the assay. Eight-point $IC_{50}$ curves for values of these molecules were determined by 3-fold dilution from the highest inhibitor concentration of either 20 or 30 μM. These experiments were performed by dispensing 100× compound solution prepared in 90% (v/v) DMSO onto the plate, followed by adding NS5-RNA complex that had been preincubated for 30 min. Reactions were initiated by the addition of BBT-ATP solution. After a 60-min incubation at room temperature, the stop solution was added, and BBT production was monitored as described above.

### *Assay miniaturization and inhibitor screening*

The assay was converted into a 384-well plate format with the reaction volume reduced to 10 μL. The reaction linearity, Z factor, S/N ratio, and $IC_{50}$ of reference compounds were examined. After miniaturization, assay performance was evaluated in a pilot screen on a compound library. The screening flowchart is presented in **Figure 1**. Each plate contained 16 wells of the total (DMSO vehicle) and blank (20 μM 3′dATP) controls in columns 23 and 24. Screening was done on 2 different days with 64 plates/batch.

### *Data analysis*

$K_m$ values were obtained by plotting the observed BBT production as a function of nucleotide or RNA concentrations, and the data were fitted to the equation $v = V_{max}$ {[substrate]/([substrate] + $K_m^{app}$)}. $IC_{50}$ values were obtained by fitting the data to a 4-parameter logistic equation, Y = Bottom + (Top − Bottom)/(1 + (10^( $logIC_{50}$ − X)^Hill slope)), where Bottom is the minimum Y value, Top is the maximum Y value, X is test compound concentration, and the Hill slope is the slope of the linear portion of the semi-log curve. $IC_{50}$ value was extrapolated from $logIC_{50}$ according to the GraphPad algorithm (GraphPad version 5; GraphPad Software, San Diego, CA). Z factor was calculated according to Zhang et al,[18] $Z = 1 - ((3SD_{Tot} + 3SD_{Min})/(mean_{Tot} - mean_{Min}))$, and compound activity was calculated from the following: % inhibition = (100 − ((sample signal − $mean_{Min}$)/($mean_{Tot}$ − $mean_{Min}$) × 100)). Screening data were uploaded into ActivityBase (IDBS, Guildford, UK) equipped with the add-in XL*fitR* (V.5, IDBS) for data normalization and visualization in Microsoft Excel and Spotfire (TIPCO, London).

## RESULTS AND DISCUSSION

To perform a high-throughput in vitro enzymatic assay for DENV NS5 RdRp, we developed FAPA. The assay principle is depicted in **Figure 2A**. The adenosine nucleotide has been modified by attaching the BBT fluorophore group to the γ-phosphate of adenosine triphosphate, resulting in a substrate named BBT-ATP. During the polymerization reaction, adenosine monophosphate is incorporated into the RNA chain, and $BBT_{PPi}$ is released as a product of the reaction. Subsequent treatment of the reaction with CIP in a high pH buffer terminates the NS5 RdRp activity and liberates the highly fluorescent BBT molecule from $BBT_{PPi}$. Measurement of the final reaction product serves as an indirect measure of RdRp activity.

We chose the BBT fluorophore to develop an HTS assay on the basis of the following criteria: it has a high extinction coefficient, a large Stokes' shift, and excellent photostability (ε = 26,484 $M^{-1}cm^{-1}$, $ex_{max}/em_{max}$ 422/566 nm). To examine BBT properties in terms of reactivity toward CIP hydrolysis, CIP reactions were optimized with AttoPhos® as the substrate mimic of the polymerase reaction by-product. Then, 5 μM AttoPhos® was treated with 0.01, 0.1, or 1 nM CIP in a total volume of 50 μL in a 96-well, half-well plate with NEB buffer no. 3 (100 mM NaCl, 10 mM $MgCl_2$, and 1 mM DTT), with pH ranging from 7.5 to 10 (Tris-HCl [pH 7.5], HEPES-NaOH [pH 8.0-8.5], AMPSO-NaOH [pH 9], and CAPSO-NaOH [pH 9.5-10]). Liberation of BBT was monitored at 422/566 nm. AttoPhos® was well hydrolyzed by CIP (see **Supplemental Figure 1 online at http://jbx.sagepub.com/supplemental**), although continuous reading beyond 10 min showed signal instability that was both CIP concentration and pH dependent. At near physiological pH, CIP was more active, but the signal was highly unstable. The CIP reaction was further optimized by performing the reaction at pH 10 in DEA buffer to drive the

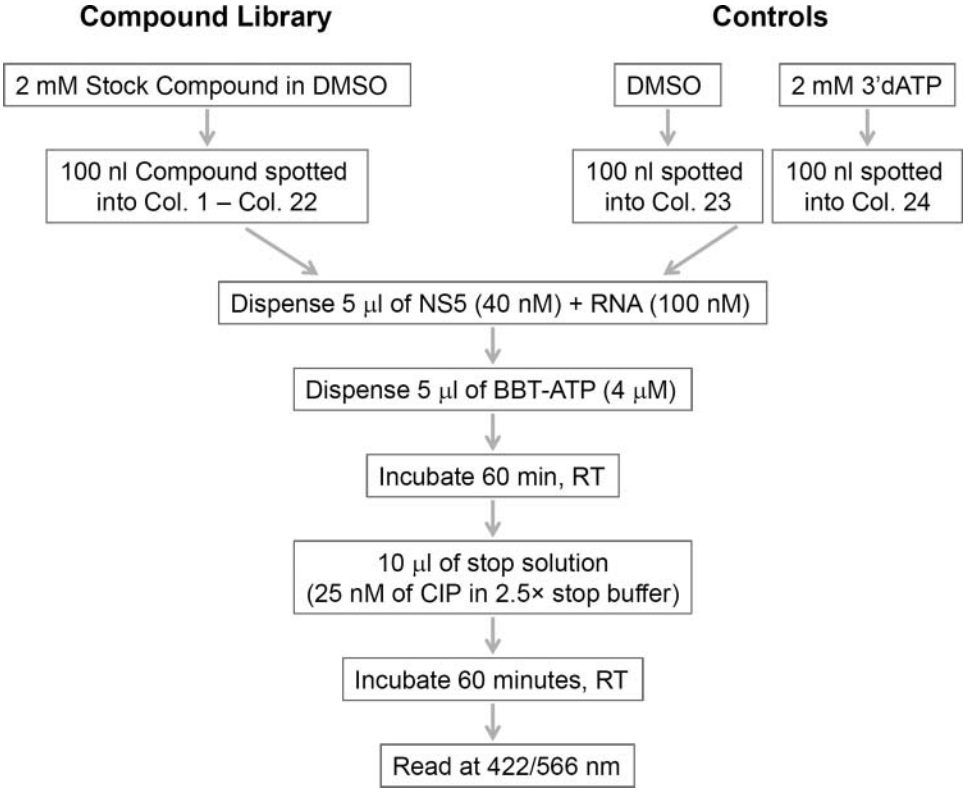


**FIG. 1.** Screening workflow of the representative library in 384-well plates. CIP, calf intestinal alkaline phosphatase; RT, room temperature.

reaction to completion through a transphosphorylation process.[19] As shown in **Figure 2B,** 1 µM AttoPhos® ($BBT_{Pi}$) was completely hydrolyzed by1 nM CIP within 1 h, and the signal remained stable up to 16 h in the buffer containing 0.5 M DEA. In addition, the RdRp substrate, BBT-ATP, is resistant to CIP hydrolysis, with its fluorescence unchanged at ~100 RFU throughout the 16-h incubation, 400-fold lower than the free form generated by the AttoPhos®-CIP reaction. Thus, the use of a high pH buffer serves 3 purposes: it inactivates DENV NS5 polymerase, promotes CIP activity, and stabilizes the fluorescent signal.

### *BBT calibration, detection limit, and assay optimization*

To ensure that the fluorescence reading from AttoPhos®-CIP treatment truly reflects the RdRp activity, calibration values were compared between BBT and AttoPhos®-catalyzed CIP reactions. BBT or AttoPhos® at 2 to 200 nM was prepared in 30 µL RdRp test buffer (50 mM Tris-HCl [pH 7.0], 50 mM NaCl, 1 mM DTT, 1 mM $MnCl_2$) before the addition of 20 µL of stop buffer containing 12.5 nM CIP (final CIP concentration at 5 nM in 50 µL). This 2-step procedure was performed to simulate the RdRp assay reaction. In addition, possible interference from the NS5 protein, RNA, and nucleotide triphosphates, which would eventually be present in the final reaction, was also investigated. CIP could hydrolyze most, if not all, the AttoPhos® in the test buffer (**Fig. 3A**). Calibration values between CIP-treated AttoPhos® and BBT were statistically similar in all the reactions tested (averaging 182 RFU/nM and 171 RFU/nM for BBT and AttoPhos®-CIP-treated reactions, respectively, $p = 0.87$). Furthermore, the presence of 20 nM NS5, 100 nM RNA, and 2 µM each of AGCU nucleotide triphosphates did not interfere with BBT fluorescence. The limit of detection was 0.5 nM (25 pmol), calculated from 3 × SD of the buffer background. Calibration curves were always determined from AttoPhos®-CIP reactions throughout the assay development process.

Assay optimization was performed in 30 µL in 96-well, half-well plates in the RdRp test buffer. We next evaluated if BBT-ATP was a substrate for the DENV NS5 RdRp. Reaction progress curves of 50 nM RdRp on either 20 nM or 100 nM 3′UTR-$U_{30}$ with 1 µM BBT-ATP are shown in **Figure 3B**. The reaction consisted of 2 steps, starting with the addition of 15 µL of 2× concentration of 3′UTR-$U_{30}$ RNA solution onto the well, followed by 15 µL of 2 × concentration of BBT-ATP. At intervals between 0 and 300 min, 20 µL of CIP in stop buffer (25 nM CIP, 200 mM NaCl, 25 mM $MgCl_2$, 1.5 M DEA) was added to inactivate RdRp and to hydrolyze the $BBT_{PPi}$. Readings at 422/566 nm were done after a 1-h incubation at room temperature to ensure complete hydrolysis of $BBT_{PPi}$ by CIP. **Figure 3B**

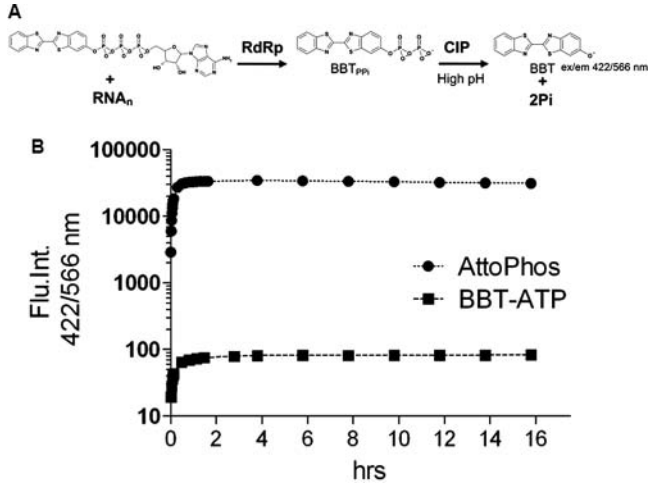


**FIG. 2.** Fluorescence-based alkaline phosphatase–coupled polymerase assay (FAPA) principle. (**A**) FAPA principle and chemical structure of BBT-ATP. RdRp catalyzes the nucleotidyl transfer of adenosine-5′ monophosphate from BBT-ATP to the growing RNA chain, generating $BBT_{PPi}$ by-products that are subsequently hydrolyzed to the highly fluorescent BBT anion ($ex_{max}$ 422 nm and $em_{max}$ 566 nm, ε, 26,484 $M^{-1}cm^{-1}$) by the calf intestinal alkaline phosphatase (CIP). (**B**) Signal stability of BBT and resistance of BBT-ATP to CIP cleavage. Either 1 μM AttoPhos® or BBT-ATP was treated with 1 nM CIP in 0.5 M deoxyethanolamine (DEA), 100 mM NaCl, 10 mM $MgCl_2$, and 1 mM dithiothreitol (DTT). AttoPhos® was completely hydrolyzed within 1 h, whereas BBT-ATP was resistant to CIP hydrolysis up to 16 h of CIP incubation.

shows that BBT-ATP was efficiently used by NS5, providing the first proof of concept of the FAPA methodology. Reaction progress curves were linear up to 80 min and beyond 200 min in the reaction containing 100 nM RNA. The signal-to-background (S/B) ratio determined at 60 min of reaction was 19.8-fold over the control reaction lacking the NS5 enzyme. Optimum enzyme and substrate concentrations were further examined with various NS5 (2.5, 5, 10, 20, and 50 nM) and RNA (10, 20, or 50 nM) concentrations. The rate of the reaction containing 20 nM NS5 was within linearity of the three RNA concentrations tested, representing good dynamic range of the assay, and was used throughout assay development. Effect of buffer components such as NaCl and KCl (ionic strength), $MgCl_2$ and $MnCl_2$ as the ion cofactor, Triton X-100 as a detergent, DTT as a reducing agent, and DMSO was investigated (data not shown). NaCl or KCl had no effect on RdRp activity, whereas $MgCl_2$ could not support RdRp activity up to 16 mM, the maximum concentration tested. We had previously investigated the effect of other divalent cations $Ca^{2+}$, $Ni^{+}$, $Co^{2+}$, and $Zn^{2+}$ on DENV-2 RdRp activity using poly(C)/oligo$(G)_{20}$ as the substrate, but none of them was able to support polymerase activity (unpublished data). The effect of $MnCl_2$ concentration and pH could not be accurately determined due to precipitation of $MnCl_2$ at alkaline pH, interfering with the fluorescent signal. However, the reaction velocity in the presence of 1 mM $MnCl_2$ at pH 7 was 40% higher than at pH 7.5, so it was selected for the RdRp assay (data not shown). NS5 RdRp can tolerate DMSO concentrations up to 1% (v/v), and inclusion of the nonionic detergent Triton X-100 at 0.01% improved enzyme activity by ~20%. We decided to use 1 mM $MnCl_2$ in the assay buffer because it could support RdRp activity. The optimized assay buffer for NS5 RdRp is 50 mM Tris-Cl (pH 7.0), 1 mM $MnCl_2$, and 0.01% Triton X-100. After obtaining optimal assay conditions, we next determined enzyme kinetics as described below.

### *FAPA for DENV-4 NS5 for HTS*

RdRp activity in the optimized buffer was linear up to 120 min in a reaction that contained 20 nM NS5, 50 nM RNA, and 2 μM BBT-ATP (**Fig. 4A**, left panel). The stop solution completely inactivated the RdRp, as demonstrated by the unchanged signal of the zero time point, where stop buffer was added to the enzyme prior to BBT-ATP. We decided to perform enzyme reactions for 60 min because this produced a sufficient window and good dynamic range with S/B and S/N ratios of 10.5 and 28.8, respectively (**Fig. 4A**, right panel).

The RdRp reaction kinetics was determined for both the 3′UTR-$U_{30}$ RNA and BBT-ATP. For the $K_m$ determinations, RNA concentrations ranging from 0 to 80 nM were assayed with a saturating BBT-ATP concentration of 20 μM or BBT-ATP concentrations ranging from 0.3 to 20 μM with 80 nM RNA. Reaction progress curves from 0 to 200 min were recorded to evaluate the reaction linearity (**Fig. 4B**, the progress curve for RNA is shown in the left panel and BBT-ATP in the right panel). We determined kinetic parameters at 60 min of reaction (percent substrate conversion <8%) because we believe that the polymerase reaction kinetics is more synchronized and represents overall nucleotide incorporation kinetics. Differences in the polymerization rate (e.g., initiation vs. elongation, abortive product formation vs. processive elongation) among flavivirus RdRp have been previously demonstrated.[20]

The $K_m$ values for 3′UTR-$U_{30}$ and BBT-ATP were 24 nM and 10 μM, respectively (**Fig. 4C**). We decided to include 50 nM RNA for screening to ensure that excess RNA would be available for the enzyme (2.5-fold excess over NS5). The $K_m^{app}$ value for BBT-ATP with 50 nM RNA was 0.75 μM. To obtain a high sensitivity assay for inhibitor finding, we decided to use 2 μM BBT-ATP in the final assay.

We next evaluated the stability of the assay reagents (see **Supplemental Figure 2**). Three conditions were tested: (1) NS5 alone, (2) NS5 incubated with RNA, and (3) NS5 incubated with BBT-ATP. Solutions of the 3 conditions were prepared at 2× concentration in 15 μL and incubated at room temperature for up to 4 h before adding 15 μL of the missing component to start the reaction (RNA + BBT-ATP, BBT-ATP

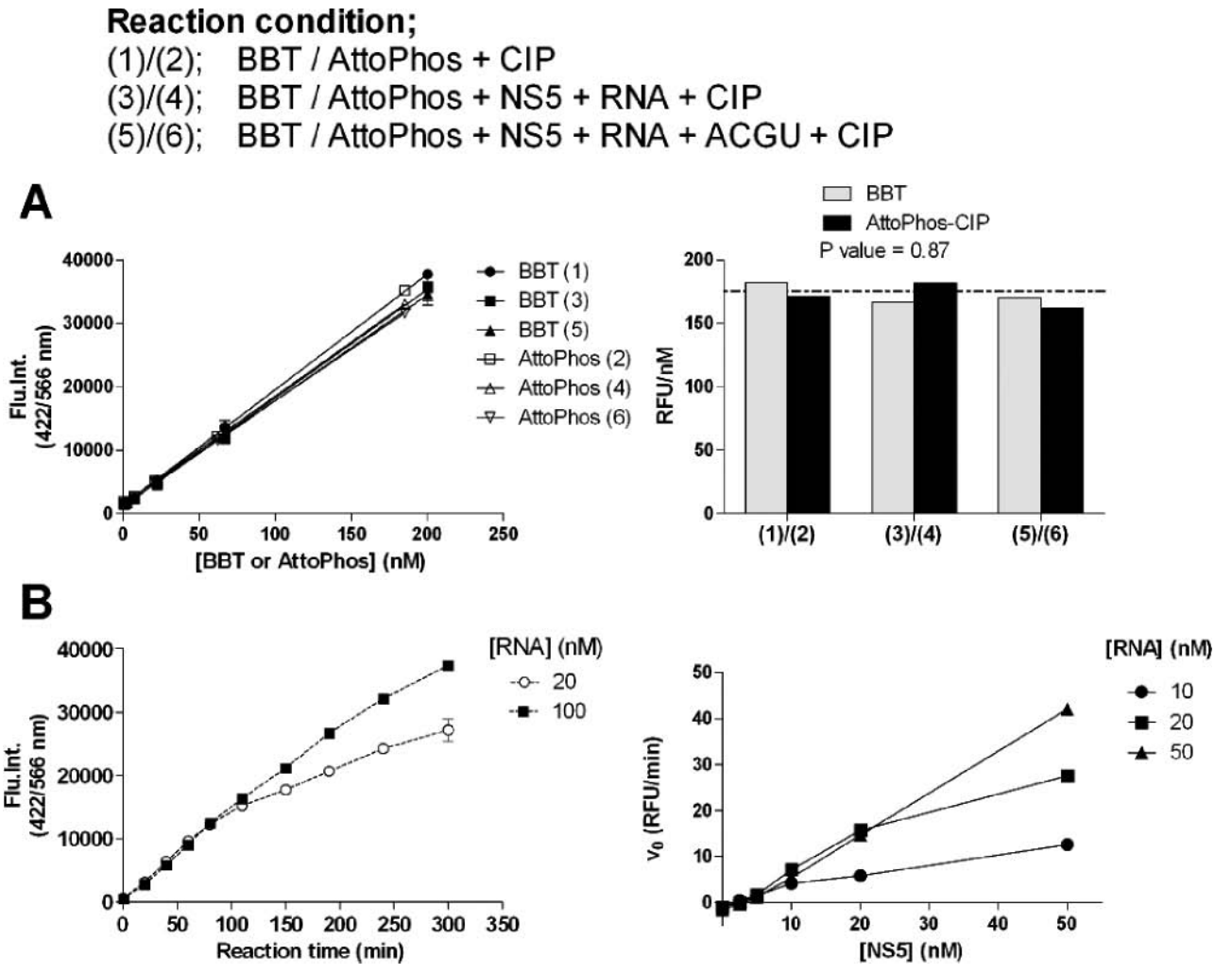


**FIG. 3.** BBT standard curve and RNA-dependent RNA polymerase (RdRp) reaction. (**A**) Standard curves determined from BBT and AttoPhos®–calf intestinal alkaline phosphatase (CIP) reactions. BBT or AttoPhos® at concentrations of 2 to 200 nM was treated with CIP (final concentration 5 nM in 50 µL), with or without NS5, RNA, and/or AGCU nucleotide triphosphates (NS5; 20 nM, RNA; 100 nM, AGCU nucleotides; 2 µM each). Each data point represents the average of triplicate wells. (**B**) RdRp reaction progress curve on the 3′UTR-$U_{30}$. Reactions were carried out with NS5 at 2.5 to 50 nM, with 10, 20, or 50 nM RNA and 2 µM BBT-ATP. Each data point represents the average from duplicated wells, with error bars indicating signal ranges.

alone, and RNA alone for reactions 1, 2, and 3, respectively). The activity of NS5 alone and NS5 with only BBT-ATP dropped slowly upon incubation in assay buffer. For NS5 alone, 10% of activity was lost after a 1-h incubation and increased to a 62% drop in activity after 4 h (compared to no preincubation). For NS5 incubated with BBT-ATP, the activity was reduced by 20% and 58% after 1- and 4-h incubations, respectively. In contrast, NS5 activity could be maintained for up to 4 h when incubated with RNA. All subsequent assays were done by preincubating NS5 with the RNA for at least 30 min before starting the experiment.

### *Validation of FAPA*

The reference compound 3′dATP and dengue adenosine nucleotide triphosphate analogue tpNITD008 were used to validate FAPA. Dose-response curves for 3′dATP and tpNITD008 are shown in **Figure 5A**. In addition, 3′dGTP was included in this study to validate the assay selectivity. The tpNITD008 was more potent than the 3′dATP, inhibiting DENV-4 NS5 RdRp with an $IC_{50}$ of 10 nM, 13-fold lower than the $IC_{50}$ of 3′dATP (127 nM). 3′dGTP did not inhibit the enzyme, indicating that the assay is specific to the polymerase

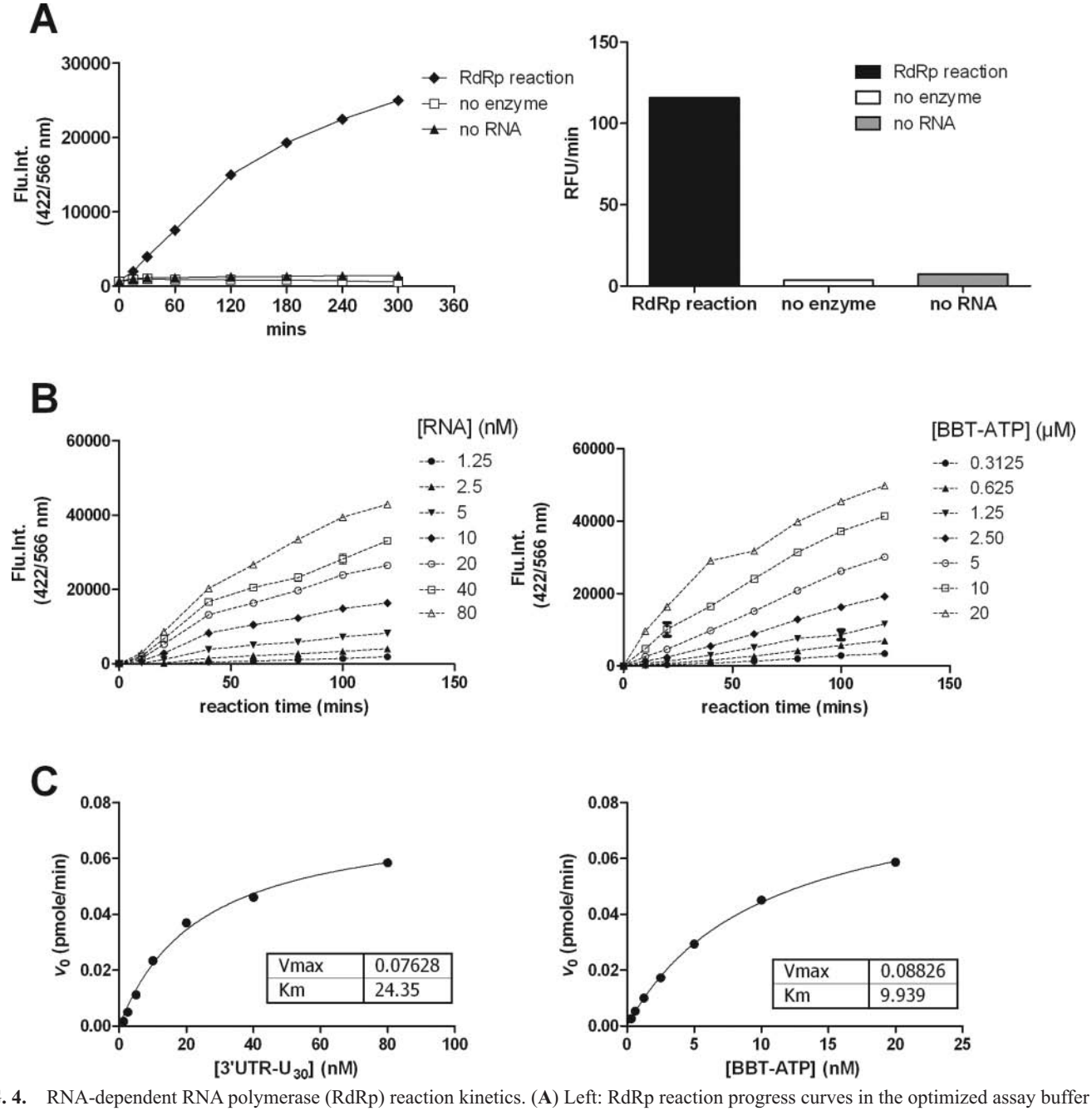


**FIG. 4.** RNA-dependent RNA polymerase (RdRp) reaction kinetics. (**A**) Left: RdRp reaction progress curves in the optimized assay buffer (50 mM Tris-Cl [pH 7.0], 1 mM $MnCl_2$, 0.01% (v/v) Triton X-100). Right: Reaction velocities of (**A**) taken from 0 to 60 min of reaction. (**B**) Reaction progress curves at various RNA and BBT-ATP concentrations. Left: RNA concentrations were between 1.25 and 80 nM, and BBT-ATP concentration was 20 μM. Right: BBT-ATP concentrations were between 0.3 and 20 μM, and RNA concentration was 80 nM. (**C**) $K_m$ for 3′UTR-$U_{30}$ and BBT-ATP. Reaction rates for the first 60 min were converted to BBT concentration calibrated from the standard curve.

reaction using adenosine triphosphate (or close analogues) as nucleotide substrates. To further validate the assay, we developed another FAPA set using a different nucleotide-RNA pair (3′UTR-$C_{30}$ and BBT-GTP). All reagents were identically prepared to that of 3′UTR-$U_{30}$ and BBT-ATP. Time course experiments showed that the reaction was linear beyond 2 h in a reaction containing 20 nM NS5, 50 nM RNA, and 2 μM BBT-GTP. The $K_m^{app}$ values for 3′UTR-$C_{30}$ and BBT-GTP under similar assay conditions were obtained at 27 nM for 3′UTR-$C_{30}$ RNA and 0.75 μM for BBT-GTP. The $K_m^{app}$ value for

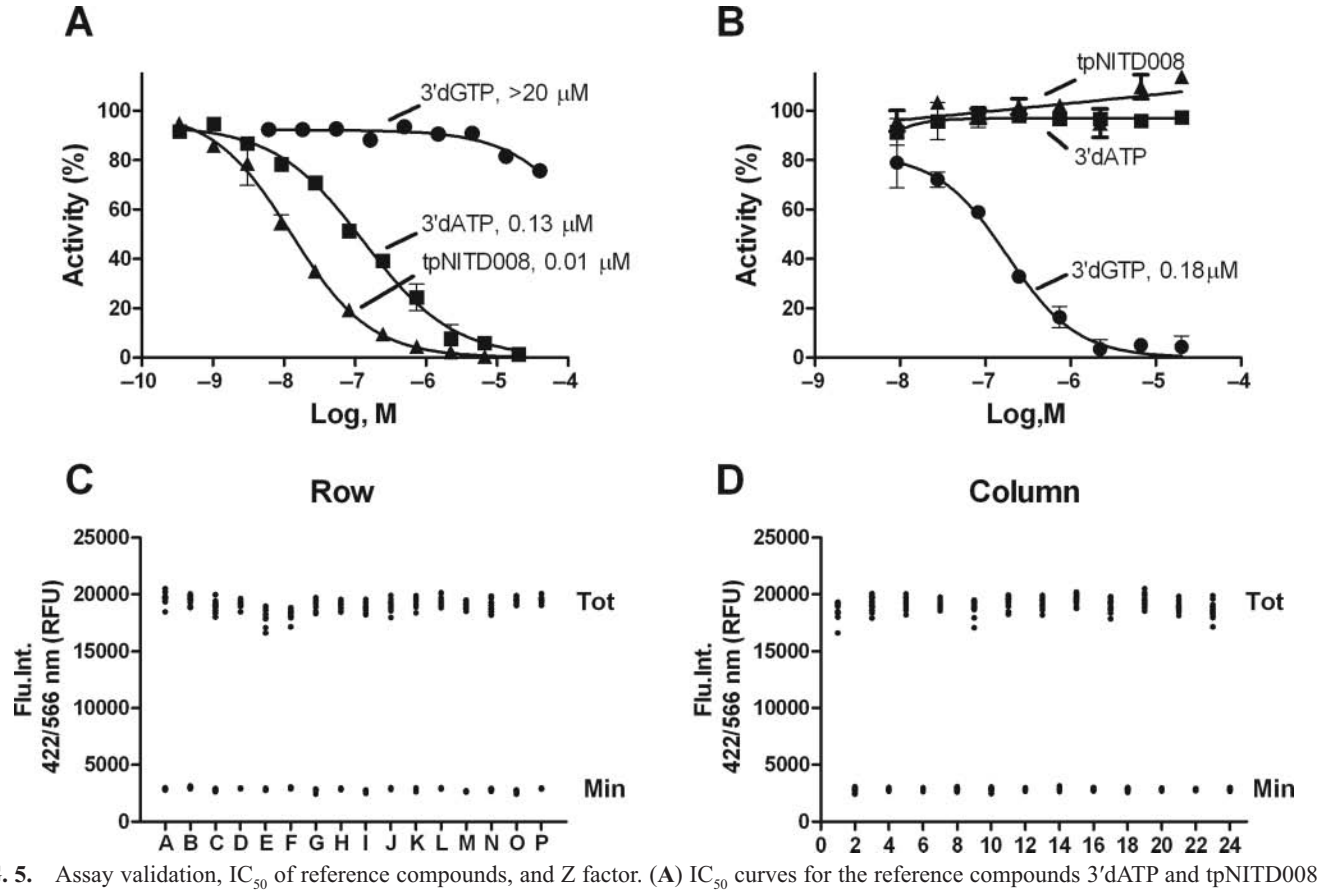


**FIG. 5.** Assay validation, $IC_{50}$ of reference compounds, and Z factor. (**A**) $IC_{50}$ curves for the reference compounds 3′dATP and tpNITD008 on the 3′UTR-$U_{30}$ and BBT-ATP substrate system. (**B**) $IC_{50}$ curves of compounds using 3′UTR-$C_{30}$ and BBT-GTP as substrates. (**C, D**) Z factors were determined with 20 nM NS5, 50 nM RNA, and 2 μM BBT-ATP in 384-well plates; 30 μM 3′dATP was used in "Min" and DMSO was used in "Tot" wells.

BBT-GTP is similar to [$^3$H]GTP used in the scintillation proximity assay (SPA).[4] Likewise, the 3′UTR-$U_{30}$ and BBT-ATP set, assay validations on 3′UTR-$C_{30}$, and BBT-GTP were performed with the 3 reference compounds 3′dGTP, 3′dATP, and tpNITD008 (**Fig. 5B**). As expected, only 3′dGTP inhibited NS5 ($IC_{50}$ 0.18 μM). These results indicate that FAPA is a versatile assay that can be adapted for other nucleotide sequences.

Assay quality was assessed by Z factor determination in 384-well plates. The reaction volume was reduced to 10 μL for the RdRp reaction and 10 μL for the stop solution, keeping the final reagent concentrations the same. The plate uniformity was tested by spotting 100 nL of 90% (v/v) DMSO as vehicle controls onto even columns ("Tot" signal) and 100 nL of 2 mM of 3′dATP (final concentration 20 μM) onto odd columns ("Min" signal) across the whole plate (**Figure 5C, D**). The Z factor calculated from the whole plate was 0.87, with an S/B ratio of 6.7 and an S/N ratio of 54. The variability of Tot and Min controls was 3.1% and 4.1%, respectively. No edge effects were observed.

**Table 1.** DENV-2, 3, 4 Kinetic Parameters and $IC_{50}$ Values of the Reference Compounds

| | *3′UTR-$U_{30}$/BBT-ATP* | | | *3′UTR-$C_{30}$/BBT-GTP* | | |
|---|---|---|---|---|---|---|
| *Substrate* | *DENV-2* | *DENV-3* | *DENV-4* | *DENV-2* | *DENV-3* | *DENV-4* |
| $K_m^{app}$ | | | | | | |
| RNA, nM | 15.25 | 15.86 | 26.74 | 21.16 | 25.59 | 24.35 |
| NTP, μM | 5.18 | 4.90 | 1.68 | 0.72 | 1.10 | 0.75 |
| $IC_{50}$, μM | | | | | | |
| 3′dATP | 0.27 | 0.15 | 0.13 | NA | NA | NA |
| 3′dGTP | NA | NA | NA | 0.28 | 0.25 | 0.29 |
| tpNITD008 | 0.12 | 0.07 | 0.01 | NA | NA | NA |

The $K_m^{app}$ values for BBT-ATP, BBT-GTP, 3′UTR-U30, and 3′UTR-C30 and $IC_{50}$ values for 3′dATP, 3dGTP, and tpNITD008 were determined under similar assay condition as described in Materials and Methods. NA, not active.

## PILOT SCREEN WITH DIVERSE COMPOUND LIBRARY

A compound library of diverse structures selected from various vendors, comprising 40,572 compounds, was used in a

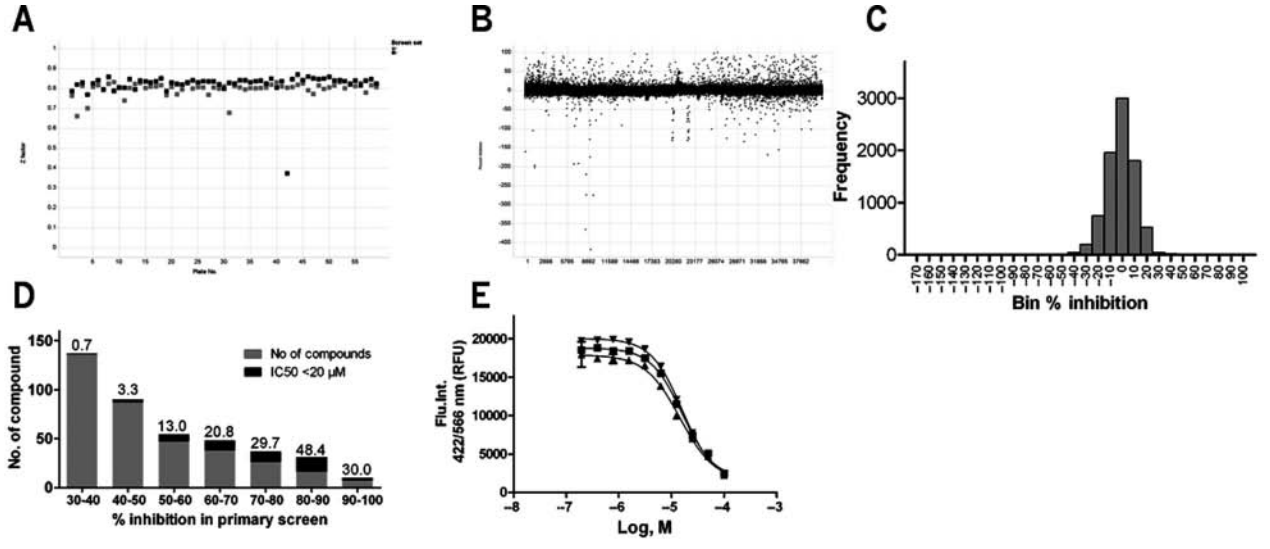


**FIG. 6.** Compound library screening. (**A**) Z factor from individual plates of the library screen. Each screen batch contained 64 plates. Data from batch 1 are in the dark circles; those from batch 2 are shown in gray. (**B**) Inhibition plot of 40,572 compounds. Compounds that showed activation (negative percent inhibition values) are likely due to signal interference. (**C**) Histogram distribution of the inhibition data. (**D**) Distribution of hits from the primary screening according to the percent inhibition and confirmation rate within each group. Hits providing $IC_{50}$ values below 20 μM were considered confirmed. The numbers on top of the bars refer to the percentage of hits that confirmed within each category. (**E**) Titration curve of a representative hit from the primary screening. Each curve corresponds to an experiment carried out on a different day.

pilot screen (118 plates in total, including 2 DMSO dummy plates). Screening (protocol is shown in **Fig. 1**) was performed in 2 batches on different days. Each assay plate contained 16 wells of Min and Tot that were used for Z factor estimation (**Fig. 6A**). Good Z factors were obtained, averaging 0.81 with an SD value of 0.05. One plate had a Z factor of 0.37 and was rejected. Percentage inhibition was calculated on a plate basis by setting average values of Tot wells as 0% inhibition. A summary of the screening results are plotted as percent inhibition and as a histogram in **Figure 6B, C**. Sample median, mean, interquartile range, and SD were 0.64, 0.72, −4.39 to 4.94, and 10.7%, respectively. Compounds with greater than 30% inhibition (calculated from 3 × SD of the sample) were selected as hits for confirmation (407 compounds total). The confirmation rate of the hits in the primary screening, ranked by potency, is shown in **Figure 6D**. A total of 50 compounds showed $IC_{50}$ values <20 μM in the confirmation assay (12.3% confirmation rate). Most of them (46 compounds) showed >50% inhibition in the primary screen (25.7% confirmation rate if a 50% cutoff were used). These compounds are under further investigation to find a lead compound for DENV NS5 RdRp. As an example, the $IC_{50}$ curves of a representative hit, determined on different days, are shown in **Figure 6E**. The 3 curves provided very close $IC_{50}$ values (12.0 μM, 9.6 μM, and 12.6 μM), evidencing the assay reproducibility and robustness.

In addition, NS5 from DENV serotypes 2 and 3 was included in this study to assess the adaptability of FAPA. To establish an assay for DENV-2 and DENV-3 NS5, we (1) determined the $K_m^{app}$ values for RNA and BBT-ATP, (2) determined the reaction linearity in a time course experiment, (3) obtained a Z factor of above 0.5, and (4) validated the assay with the 3′dATP reference compound. The kinetic parameters for DENV NS5 serotypes 2 and 3 and $IC_{50}$ values for inhibitors are shown in **Table 1**. All 3 DENV NS5 had similar affinity to RNA substrates ($K_m^{app}$ for 3′URT-$U_{30}$ or 3′UTR-$C_{30}$; 15.25-26.74 nM), whereas the binding affinity for BBT-GTP was higher than that for BBT-ATP. The ratios of the $K_m^{app}$ values of BBT-ATP/BBT-GTP were DENV-2, 7.2-fold; DENV-3, 4.5-fold; and DENV-4, 2.2-fold. 3′dGTP had similar inhibition potency against all serotypes ($IC_{50}$ 0.25-0.28 μM), whereas 3′dATP had ~2-fold lower potency against DENV-2 ($IC_{50}$ 0.27 μM) compared with DENV-3 or DENV-4 ($IC_{50}$ 0.15 and 0.13 μM, respectively), as well as the tpNITD008, which inhibited DENV-2 with an $IC_{50}$ of 0.12 μM, 2- and 11.6-fold higher than DENV-3 and DENV-4, obtained at 0.07 and 0.01 μM, respectively.

In summary, the FAPA is versatile, homogeneous, and robust. The method presented here should allow the screening of compounds targeting polymerases. The assay is robust enough to avoid identifying nonspecific inhibitors commonly detected in an HTS, facilitating the drug discovery process by identifying inhibitors that are specific to the polymerase protein target.

## ACKNOWLEDGMENT

We thank Shamala Devi for providing RNA viruses for cloning of DENV-3 and DENV-4 NS5. In addition, we thank Shahul Nilar for compound selection, Amelia Yap and Wan

Kah Fei for help with screening, and Christian Noble for help in manuscript editing.

## REFERENCES


1. Courageot MP, Frenkiel MP, Dos Santos CD, Deubel V, Despres P: Alpha-glucosidase inhibitors reduce dengue virus production by affecting the initial steps of virion morphogenesis in the endoplasmic reticulum. *J Virol* 2000;74:564-572.
2. Diamond MS, Zachariah M, Harris E: Mycophenolic acid inhibits dengue virus infection by preventing replication of viral RNA. *Virology* 2002;304:211-221.
3. Zhang XG, Mason PW, Dubovi EJ, Xu X, Bourne N, Renshaw RW, et al: Antiviral activity of geneticin against dengue virus. *Antiviral Res* 2009;83:21-27.
4. Yin Z, Chen YL, Kondreddi RR, Chan WL, Wang G, Ng RH, et al: N-sulfonylanthranilic acid derivatives as allosteric inhibitors of dengue viral RNA-dependent RNA polymerase. *J Med Chem* 2009;52:7934-7937.
5. Whitby K, Pierson TC, Geiss B, Lane K, Engle M, Zhou Y, et al: Castanospermine, a potent inhibitor of dengue virus infection in vitro and in vivo. *J Virol* 2005;79:8698-8706.
6. Yin Z, Chen YL, Schul W, Wang QY, Gu F, Duraiswamy J, et al: An adenosine nucleoside inhibitor of dengue virus. *Proc Natl Acad Sci U S A* 2009;106:20435-204359.
7. Schul W, Liu W, Xu HY, Flamand M, Vasudevan SG: A dengue fever viremia model in mice shows reduction in viral replication and suppression of the inflammatory response after treatment with antiviral drugs. *J Infect Dis* 2007;195:665-674.
8. Hanley KA, Lee JJ, Blaney JE Jr, Murphy BR, Whitehead SS: Paired charge-to-alanine mutagenesis of dengue virus type 4 NS5 generates mutants with temperature-sensitive, host range, and mouse attenuation phenotypes. *J Virol* 2002;76:525-531.
9. Ray D, Shah A, Tilgner M, Guo Y, Zhao Y, Dong H, et al: West Nile virus 5′-cap structure is formed by sequential guanine N-7 and ribose 2′-O methylations by nonstructural protein 5. *J Virol* 2006;80:8362-8370.
10. Egloff MP, Benarroch D, Selisko B, Romette JL, Canard B: An RNA cap (nucleoside-2′-O-)-methyltransferase in the flavivirus RNA polymerase NS5: crystal structure and functional characterization. *EMBO J* 2002;21: 2757-2768.
11. Dong H, Ren S, Zhang B, Zhou Y, Puig-Basagoiti F, Li H, et al: West Nile virus methyltransferase catalyzes two methylations of the viral RNA cap through a substrate-repositioning mechanism. *J Virol* 2008;82:4295-4307.
12. Nomaguchi M, Ackermann M, Yon C, You S, Padmanabhan R: De novo synthesis of negative-strand RNA by dengue virus RNA-dependent RNA polymerase in vitro: nucleotide, primer, and template parameters. *J Virol* 2003;77:8831-8842.
13. Yap TL, Xu T, Chen YL, Malet H, Egloff MP, Canard B, et al: Crystal structure of the dengue virus RNA-dependent RNA polymerase catalytic domain at 1.85-angstrom resolution. *J Virol* 2007;81:4753-4765.
14. Wang YK, Rigat KL, Roberts SB, Gao M: A homogeneous, solid-phase assay for hepatitis C virus RNA-dependent RNA polymerase. *Anal Bio* 2006;359:106-111.
15. Bhat J, Rane R, Solapure SM, Sarkar D, Sharma U, Harish MN, et al: High-throughput screening of RNA polymerase inhibitors using a fluorescent UTP analog. *J Biomol Screen* 2006;11:968-976.
16. Kozlov M, Bergendahl V, Burgess R, Goldfarb A, Mustaev A: Homogeneous fluorescent assay for RNA polymerase. *Anal Biochem* 2005;342:206-213.
17. Simpson D, Daily B, Brehm S: The AttoPhos® system for fluorescent detection of alkaline phosphatase in an enzyme-linked assay [Online]. Retrieved from http://www.promega.com/pnotes/74/8414_07/8414_07.html
18. Zhang JH, Chung TD, Oldenburg KR: A simple statistical parameter for use in evaluation and validation of high throughput screening assays. *J Biomol Screen* 1999;4:67-73.
19. McComb BR, Bowers GN Jr: Study of optimum buffer conditions for measuring alkaline phosphatase activity in human serum. *Clin Chem* 1972;18:97-104.
20. Selisko B, Dutartre H, Guillemot JC, Debarnot C, Benarroch D, Khromykh A, et al: Comparative mechanistic studies of de novo RNA synthesis by flavivirus RNA-dependent RNA polymerases. *Virology* 2006;20:145-158.


Address correspondence to:
*Yen-Liang Chen*
*Novartis Institute for Tropical Diseases*
*10 Biopolis Road, #05-01 Chromos, Singapore 138670*

*E-mail:* yen_liang.chen@novartis.com